

Phase separation of phospholipid multilayers incorporated with cell penetrating peptides

Huaiyu Jing, Heesuk Kim, and Dongjin Choi

Department of Chemistry and Interdisciplinary Program of Integrated Biotechnology, Institute of Biological Interfaces, Sogang University, Seoul 121-742, Korea

Dong Ryeol Lee

Department of Physics, Soongsil University, Seoul 156-743, Korea

Jeong Soo Lee

Korea Atomic Energy Research Institute, Yuseong, Daejeon 305-600, Korea

Chung-Jong Yu

Pohang Accelerator Laboratory, POSTECH, Pohang 790-784, Korea

Kwanwoo Shin^{a)}

Department of Chemistry and Interdisciplinary Program of Integrated Biotechnology, Institute of Biological Interfaces, Sogang University, Seoul 121-742, Korea

(Received 30 March 2011; accepted 24 May 2011; published 29 June 2011)

We used X-ray reflectivity to investigate the structures of phospholipid multilayers with transcription-activating-factor-derived peptide (TDP) as a function of the membrane charge density. Mixed phospholipid multilayers of 1,2-dipalmitoyl-sn-glycero-3-phosphocholine (DPPC) and 1,2-dipalmitoyl-sn-glycero-3-phosphoserine (DPPS) with different mixing ratios (C:S) were used to elucidate the various charge densities in a plasma membrane. We fixed the peptide/lipid molar ratio (P/L) and varied the DPPC/DPPS molar ratio in the mixed multilayer. In the pure DPPC multilayer, the incorporation of TDP had nearly no effect on the bilayer thickness of the mixed lipid multilayer. However, in the mixed DPPC/DPPS multilayer, the incorporation of TDP decreased the bilayer thickness, suggesting that the TDP peptide had a stronger interaction with DPPS than with DPPC and caused disorder in the lamellar structure. Combining this with the refined X-ray reflectivity (XR) data, we concluded that the TDP existed more in the headgroup region of the TDP-induced segregated DPPS in the mixed multilayer and caused significant membrane thinning. © 2011 American Vacuum Society. [DOI: 10.1116/1.3602087]

I. INTRODUCTION

Phase behaviors of phospholipids in plasma cell membranes, such as phase separation and lateral de-mixing of phospholipids, have been known to be key physical phenomena, related to the assembly of signaling molecules, the nucleation of transient pores and membrane protein trafficking, for which phospholipid raft domains are mainly responsible.¹⁻⁴ Key factors in phase behavior are, in general, i) the length and the property of phospholipid tails, from which the fluidity and the strength of the attractive van der Waals interactions between lipid molecules can be determined,^{5,6} ii) the composition of charged phospholipid headgroups, in which the electrostatic interaction between adjacent lipids stabilizes or disrupts the lipid membranes,^{7,8} and iii) various types of embedded biological molecules, such as cholesterol, membrane proteins, and glycosphingolipids, which are known to be major components, in addition to phospholipids of the lipid raft domain.⁹

When charged extracellular macromolecules are introduced into the membranes, the phase behaviors of lipid membranes become even more complicated. In fact, the formation of lipid-extracellular molecule complexes has been

shown in various morphologies. For examples, Safinya and his group found that anionic DNA molecules induced in-plane mobility of counter ionic lipid molecules, yielding a lamellar phase.^{10,11} They also reported an inverted hexagonal phase when anionic molecules were bound to counter-ionic lipid molecules.¹² Although many biological applications, including a non-viral delivery in a gene delivery system and a biosensor system, require a good understanding of the phase stability and of the interaction mechanism of phase separation domains in biological membranes, the phase behaviors of lipid membranes, particularly when they are interacting with charged extracellular molecules, are poorly understood.

Recently, we reported the structures of phospholipid multilayers consisting of neutral (DPPC) and anionic (DPPS) phospholipids as a function of the lipid composition and found that, based on X-ray reflectivity measurements, no macroscopic phase separation, in the absence of cations, occurred under both dry and humid conditions.¹³ However, by observing cation-chelated lipid solid aggregates, Taguchi and Wakayama found that phase separation could be induced by multivalent cations (Ca²⁺) in the DPPS (1,2-dipalmitoyl-sn-glycero-3-phosphoserine)/DPPC (1,2-dipalmitoyl-sn-glycero-3-phosphocholine) bilayers.¹⁴ Furthermore, Huang's group used X-ray diffraction to investigate extensively

^{a)}Electronic mail: kwshin@sogang.ac.kr

the peptide-induced membrane thinning mechanism for a stack of parallel lipid bilayers on a solid substrate and found that the thickness of the lipid bilayer decreased linearly with increasing peptide-lipid molar ratio (P/L) and that the membrane thinning effect was mainly responsible for the pore formation that occurred when the lipid membranes interacted with α -helical antimicrobial peptides, e.g., alamethicin, and melittin.^{15,16} Instead of multivalent ions or amphiphilic α -helical rods, we investigated the phase behaviors of mixed lipid multilayers with highly positively charged cell-penetrating peptides (CPPs), which are a class of short peptide sequences that can traverse cell membranes efficiently, incorporated.¹⁷ CPPs are often used as transporters for various biological drugs such as peptides, proteins, and genes, which are attached as cargo. The transcription-activating-factor-derived peptide (TDP), which has 11 key amino acid residues with mostly lysine and arginine (YGRKKRRQRRR) from the human immunodeficiency virus (HIV-1) TAT protein, has been used as the CPP for incorporation into the phospholipid multilayer.¹⁸ TDP is the most widely studied CPP and is known to be an essential viral regulatory factor and a nucleus localization agent.¹⁹ This study was conducted to determine whether TDP molecules could also induce lipid phase separation and lateral demixing, which might be responsible for segregated domains, nucleation of transient pores, raft domains, and so on.

In this work, DPPC, a representative of the most abundant zwitterionic phosphatidylcholines (PC) in human cell membranes, and DPPS, a representative of net-negatively-charged phosphatidylserines (PS), the most important components in mammalian cell membranes, were used as the lipid components.²⁰⁻²² Substrate-supported lipid/CPP multilayers, with TDP being used as the CPP, were prepared by using the self-assembled method, and the structures of the mixed lipid multilayers with TDP incorporated were explored. We varied the DPPC-to-DPPS molar ratio while keeping the DPPC content fixed and changing the DPPS content, and we compared the structure of the lipid/TDP mixed multilayer with that of the mixed lipid multilayer without TDP for various contents of DPPS (net-negatively-charged lipids) by using X-ray reflectivity. With increasing DPPS content, the bilayer thickness of the lipid/TDP multilayer became thinner, and a DPPC/DPPS phase separation induced by the incorporation of TDP was observed. The results suggest that TDP, which has a strong electrostatic interaction with DPPS, induces a strong binding phenomenon, resulting in a phase separation within the mixed lipid multilayers.

II. MATERIALS AND METHODS

Synthesized transcription-activating-factor-derived peptide (TDP) with a sequence corresponding to YGRKKRRQRRR was purchased from Anygen, Co. (Korea). DPPC and DPPS were purchased from Avanti Polar Lipids and were used without further purification. P-type (100), single-side-polished silicon wafers were used as substrates. The silicon wafers were thoroughly cleaned in a piranha solution and hydrophilically treated. TDP was dis-

solved in distilled water, and DPPC and DPPS in different molar ratios ($C/S=1:0, 7:3, 3:7, \text{ and } 0:1$), keeping the DPPC content fixed while varying the DPPS content, were first dissolved in a mixture of methanol and chloroform ($v:v=1:1$). The lipid solutions were then mixed with the TDP aqueous solution. Throughout the experiments, we fixed the peptide/lipid molar ratio (P/L) to be $1/200$. We pipetted the mixed solution onto the silicon substrate in a closed chamber. The solution spread spontaneously, and the solvent evaporated slowly over a period of 6 h. The samples were then kept in a vacuum desiccator for another 12 h to get rid of any residual solvent.²³

X-ray reflectivity (XR) measurements were taken at the 5C2 K-JIST beamline of the Pohang Accelerator Laboratory at an energy of 10 keV, which corresponds to a wavelength of $\lambda=1.24 \text{ \AA}$. The XR was measured by scanning the incident angle θ to the sample's surface with respect to the direction of the primary beam and by simultaneously moving the detector arm by 2θ . For the specular reflection, the wave vector transfer q_z is only in the z -direction, which is normal to the sample's surface. The specular reflectivity was defined as the intensity as a function of q_z for various incident θ_i and exit θ_f while maintaining $\theta_i=\theta_f$. Since $q_x=q_y=0$, θ is given by $q_z=(4\pi/\lambda)\sin\theta$. The structural parameters of the lipid multilayers were the layer thicknesses, the electron density contrast, and the interfacial roughness. In order to obtain more information on the multilayers, we obtained the electron density profiles by fitting the X-ray reflectivity data, which could be refined via

$$\rho(z) = \sum_1^N f(q_{z,m}) \cos(2\pi mz/d), \quad (1)$$

where $f(q_{z,m})$ is the form factor of the bilayer, d is the period of the multilayer (peak-to-peak distance), and the m , running from 1 to N , are the indices of the Bragg peaks. The magnitudes of $f(q_{z,m})$ are determined by the intensities of the Bragg peaks:

$$I(q) \propto \left| \sum_{n=0}^{N+1} f_n e^{iq_z n d} \right|^2 / q_z^2, \quad (2)$$

where $f_0=f_S$ is the reflection of the substrate and $f_{N+1}=f_a e^{-iq_z d}$ (f_a is the form factor of the mean electron density of the film). Due to the mirror plane symmetry of the bilayers, the phases of $f(q_{z,m})$ are reduced to their positive/negative signs only, facilitating the phase problem.^{13,24,25}

III. RESULTS AND DISCUSSION

The lamellar structure DPPC/DPPS mixed lipid multilayers with TDP incorporated were investigated by using XR under humid conditions. In Fig. 1(a), we plot the specular X-ray reflectivity measurements as a function of q_z for lipid multilayers formed on hydrophilic Si wafers. The different curves correspond to different molar ratios of DPPC to DPPS, $C:S=1:0, 7:3, 3:7, \text{ and } 0:1$ (from bottom to top), with TDP incorporated at a fixed TDP/lipid ratio (P/L) of $P/L=1/200$ for all samples. Here, we should note that the P/L of $1/200$, which is lower than that of previous

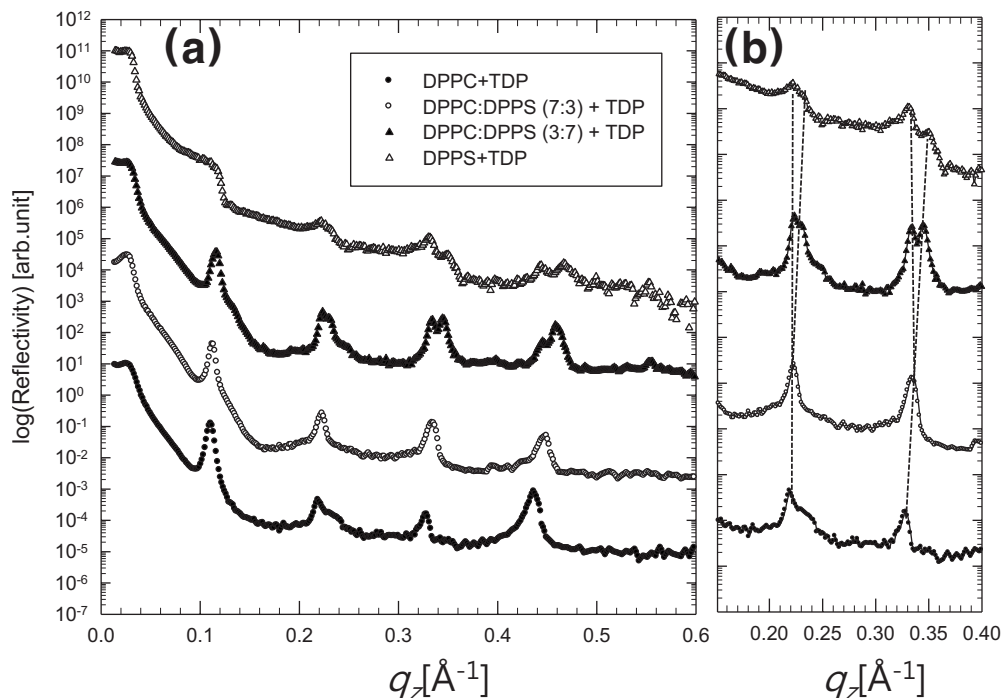


FIG. 1. (a) X-ray reflectivity curves as a function of q_z for lipid multilayers formed on hydrophobic Si wafers. The different curves correspond to different molar ratios of DPPC and DPPS, $C:S=1:0, 7:3, 3:7, 0:1$ (from bottom to top), with TDP incorporated at $P/L=1/200$ for all samples. The curves were offset by a constant for easier viewing. (b) Magnified curves of the positions of the 2nd- and the 3rd-order peaks in Fig. 1(a). The vertical dashed lines demonstrate that the Bragg peaks separate with increasing content of DPPS.

research,^{15,16} was intentionally chosen in this experiment for several reasons. First, pore formation often occurs for $P/L > 1/100$ for many antimicrobials. At lower P/L , peptide molecules bonded to a membrane are considered to be parallel to the plane of the membrane. For example, mellitin begins to penetrate into the membrane at $P/L > 100$, and two different states (the S state and the I state) of the peptide coexist.¹⁵ Second, the presence of peptides parallel to the membrane is highly sensitive to the membrane's thickness. Once the P/L ratio becomes larger than its critical $(P/L)^*$, then the membrane's thickness becomes insensitive to the P/L ratio due to a structural conversion from the S state to the I state, yielding a peptide orientation perpendicular to the plane of the membrane.

From Fig. 1(a), we can see that the XR data exhibit clearly resolved Bragg peaks at high- q_z regions, indicating that lipid/TDP layers are periodically stacked from the substrate. The electron density profiles constructed from the XR data are shown in Fig. 4, and we are interested in the interlayer spacings, d , from headgroup to headgroup, which can be readily obtained from the difference between the frequencies of the Bragg peaks (Δq_z) for each spectrum by using $d=2\pi/\Delta q_z$. For the DPPC/TDP multilayer, regularly-spaced single-frequency Bragg peaks are shown, indicating that the sample retains a DPPC/TDP multilayer with a single period. When we increased the $C:S$ ratio to 7:3, the single-frequency Bragg peaks were still maintained, indicating that DPPC and DPPS were mixed homogeneously. When 70% DPPS was mixed into DPPC, the 2nd, 3rd, and 4th Bragg peaks were separated into 2 peaks. The presence of two competing fre-

quencies in one scan strongly implies that at least two different lamella periods are present. The peak separation was more distinct for pure DPPS ($C:S=0:1$). The decreased peak intensities and the broadened peak widths in the patterns for $C:S=3:7$ and $0:1$ suggest that the incorporation of the TDP destroyed the homogeneously-layered lipid structure.

We saw obvious structural changes after the incorporation of positively charged TDP. Previously, we reported that only a single-frequency Bragg peak was observed for multilayers with DPPC/DPPS lipid ratios of 1:0, 7:3, 3:7, and 0:1 without the incorporation of TDP.¹³ In that paper, we concluded that no macroscopic phase separation occurred when two lipids were mixed. However, when TDP molecules were incorporated in this experiment, a separation of the Bragg peaks was observed for the DPPS-rich samples, $C:S=3:7$ and $0:1$. Figure 1(b) shows the effect of DPPS content on the separation of the Bragg peaks. Figure 1(b) magnifies the positions of the 2nd- and the 3rd-order peaks, for which a single peak is separated into two. For example, the 2nd-order Bragg peak at $\sim 0.22 \text{ \AA}^{-1}$ is nearly constant for all samples, but for $C:S=3:7$ and $0:1$, peaks appear at $\sim 0.23 \text{ \AA}^{-1}$ and $\sim 0.24 \text{ \AA}^{-1}$, respectively.

In Fig. 2, we plot d obtained from $d=2\pi/\Delta q_z$ for various of $C:S$ ratios. When the molar ratios of DPPS > 0.7 , a secondary d spacing is visible. Together with d (closed circles) obtained from Fig. 1, we also plotted the reported values (open circles) of interlayer spacings, which were obtained for lipid multilayers without the incorporation of TDP.¹³ From the figure, one can see that the pure DPPC and the DPPC/

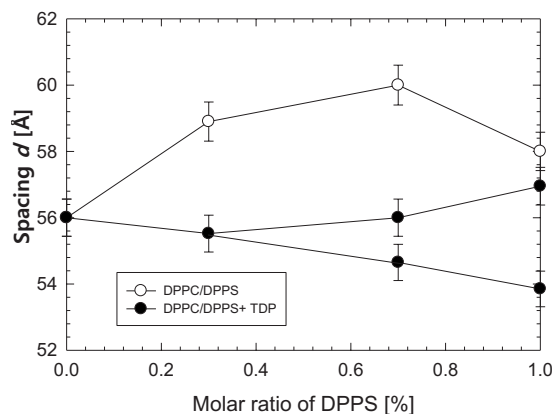


FIG. 2. Variation of the headgroup-to-headgroup spacings for the DPPC/DPPS lipid multilayer before (○) and after (●) the incorporation of TDP as a function of the DPPS molar ratio. Interlayer spacings for lipid multilayers without the incorporation of TDP were excerpted from the values (open circles) reported in Ref. 11.

TDP multilayer have almost the same bilayer thicknesses, indicating that the incorporation of the TDP has negligible effect on the bilayer thickness of the DPPC multilayer at our P/L ratio ($P/L=1/200$). With increasing $C:S$ ratio from 0 to 0.3 in the mixed lipid, the bilayer thickness decreases slightly. A TDP-induced DPPC/DPPS phase separation is obvious at $C:S=3:7$. From Fig. 2 and the guideline in Fig. 1(b), we can see that the bilayer thickness of the lipid/TDP multilayer decreases from 58.9 Å to 55.5 Å as the $C:S$ ratio is changed from 1:0 to 7:3. When the $C:S$ ratio is increased

to 3:7, we see two obvious spacings in the XR pattern. The bilayer thickness of the lipid/TDP multilayer decreases from 60.0 Å for the single spacing to 56.0 and 54.4 Å for the second spacing. After the DPPC and the DPPS had a phase separation, the bilayer thickness of the first spacing was almost the same as that of pure DPPC, and the second spacing could be attributed to the TDP-incorporated DPPS multilayer. All these results indicate that TDP has stronger interactions with negatively charged DPPS than with neutral DPPC due to electrostatic interactions.

From the results shown in Figs. 1 and 2, one can suggest one possible structure of the mixed lipid/TDP multilayer; the TDP molecules interact with charged lipid headgroups and are condensed between the hydrophilic headgroup regions of the lipid multilayer. When antibacterial peptides are bound to lipid membranes, membrane thinning is often observed, suggesting that the peptides embedded in the headgroup are stretching the lipid molecules in a direction parallel to the substrate. Pore formation induced by the TDP molecules is not expected at this low P/L ratio.^{26–29} Therefore, membrane thinning, if it occurs upon the binding of TDP to the lipid membrane, must be due to TDP localized near DPPS lipids because the total lipid per peptide ratio is constant. If more peptide molecules are localized near DPPS, then the P/L ratio for the localized peptide-to-DPPS ratio has to be higher than that for the peptide-to-total lipid (DPPC+DPPS) ratio. As the molar ratio of DPPS is low (e.g., 7:3), the lipid membranes may not be segregated upon binding with TDP molecules. As the molar ratio of DPPS increases, however, the

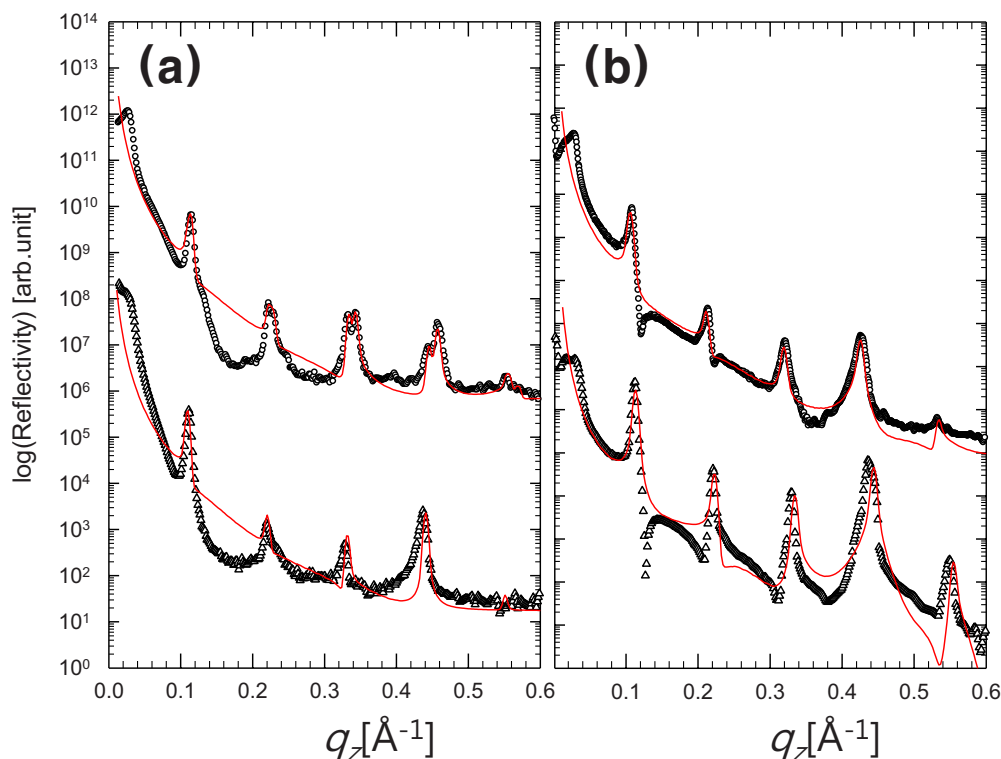


FIG. 3. (Color online) Observed and refined (—) X-ray reflectivity profiles (a) of the mixed DPPC/DPPS multilayer with a $C:S$ ratio of 3:7 and (b) of the DPPC before (open triangles) and after (open circles) the incorporation of the TDP peptide ($P/L=1/200$).

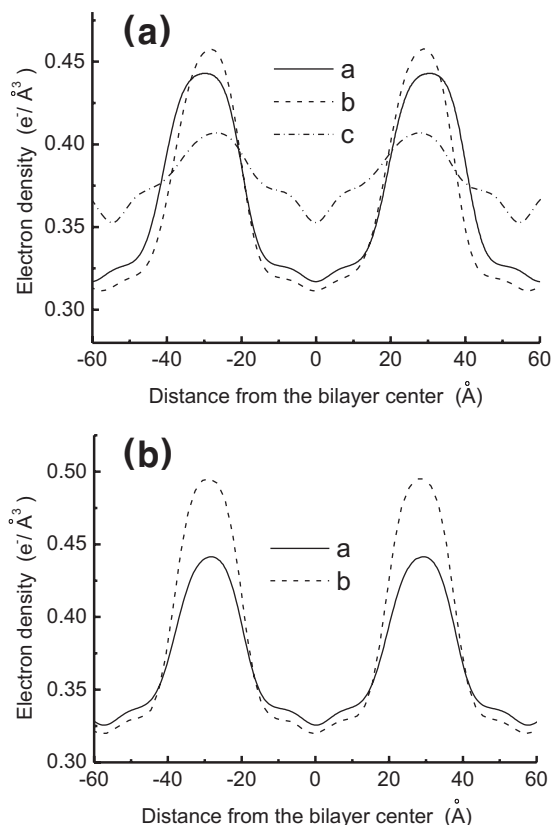


FIG. 4. Corresponding electron density models used to fit the observed X-ray reflectivity data in Fig. 3. (a) Electron density profiles of the mixed DPPC/DPPS multilayer with a C:S ratio of 3:7 before (line) and after (dashes and dash-dots) the incorporation of the TDP peptide. (b) Electron density profiles of the DPPC multilayer before (line) and after (dashes) the incorporation of the TDP peptide.

TDP molecules may induce DPPS segregation as a result of preferred TDP binding to the DPPS headgroup. In this case, we have to consider different P/L ratios up to highly-rich-TDP-to-DPPS ratios and up to normal TDP-to-DPPC ratios, the former will result in more serious membrane thinning while the latter will not, with the same thickness being maintained.

Figures 3(a) and 3(b) depict the observed and the refined (—) reflectivity profiles of the mixed DPPC/DPPS multilayer with a C:S ratio of 3:7 [Fig. 3(a)] and the DPPC [Fig. 3(b)] before (open triangles) and after (open circles) the incorporation of the TDP peptide ($P/L=1/200$). The corresponding electron density profiles derived from the XR patterns for Figs. 3(a) and 3(b) are shown in Figs. 4(a) and 4(b), respectively. For the XR pattern with two spacings (Fig. 3(a)), we derived two different density profiles [Fig. 4(a)] and then cooperatively combined them into a single refined curve. As shown in Fig. 4(a), two independent electron density profiles (b and c) were derived from the best fitting model for the two competing Bragg peaks observed for the mixed DPPC/DPPS multilayer with a C:S ratio of 3:7 after the incorporation of the TDP peptide; One of the profiles, (b), corresponds to the DPPC multilayer, and the other (c) is for the mixed DPPS/TDP multilayer. Compared with the mixed DPPC/TDP

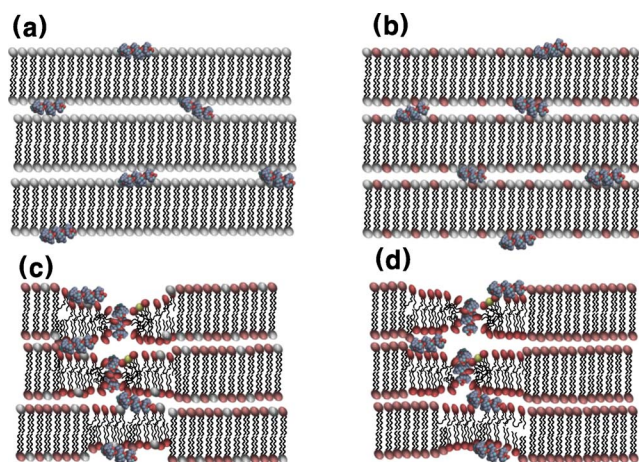


FIG. 5. (Color online) Schematic models of TDP incorporated lipid multilayers with different molar ratios of DPPC and DPPS, (a) C:S=1:0, (b) 7:3, (c) 3:7, and (d) 0:1. Note that localization of TDP at the headgroup regions of the DPPS induces membrane thinning and pore formation, resulting in vertically inserted TDP states (c and d).

multilayer, one of the obvious differences in the electron density profile is that the bilayer thickness of the lipid/TDP multilayer decreased from 60.0 Å for the single spacing to 56.0 Å for the first spacing and 54.4 Å for the second spacing.

According to Ref. 30, the electron density of a protein is lower than that of the lipid headgroup, but higher than that of the hydrocarbon chain; therefore, after the incorporation of the TDP, the increased averaged electron density of the lipid tail layers indicates that the electron density of TDP molecules is somewhat added into that of the hydrocarbon tails. The results can be explained only if the peptides adsorbed at the surface transform to a form perpendicular to the plane of the membrane. Since a preferred binding affinity of the TDP to anionic DPPS headgroup is expected, the TDPs, then, must be localized at a DPPS-rich area, forming pores in which the TDP can exist perpendicular to the plane of the lipid layers.^{26–28} Since the P/L ratio is too low to create pores throughout the given lipid systems, two different microscopic phases having different DPPS compositions are formed for the mixed DPPC/DPPS multilayer with a C:S ratio of 3:7.

From the refined data for the DPPC/TDP multilayer [Fig. 3(b)], we can see that the electron density [Fig. 4(b)] of the headgroup layer increases from 0.44 to 0.49 $e^-/\text{Å}^3$ after the incorporation of TDP, which can be attributed to the incorporation of TDP only in the headgroup region. Since there was no serious change in the interlayer thickness, the membrane thinning effect due to TDP incorporation at $P/L=1/200$ is negligible for the lipid structure of the pure DPPC membrane.

The proposed TDP incorporation models in the DPPC/DPPS mixed lipid multilayers can be summarized as schematically shown in Fig. 5. At low DPPS compositions (C:S=1:0 and 7:3), TDPs are embedded in a form parallel to the plane of the lipid membranes (Figs. 5(a) and 5(b), respectively). Due to the relatively low (or no) DPPS com-

position, no lateral demixing of the DPPS molecules in a DPPC matrix occurred; consequently, only a single phase was observed. At high DPPS compositions ($C:S=3:7$ and $0:1$), however, the positively charged TDP attracts the neighboring anionic DPPS molecules, yielding laterally-segregated TDP-binding DPPS-rich-regions (Figs. 5(c) and 5(d), respectively). The increased TDP concentration at the peptide-binding DPPS rich regions might further induce the formation of TDP-incorporated pores (i.e., toroidal model²⁹), causing the inserted state of TDP to have an orientation perpendicular to the plane of the lipid membranes.

IV. CONCLUSIONS

The structural variation in the mixed lipid/TDP multilayers as a function of the charge density was investigated by using X-ray reflectivity. Compared with the homogeneously mixed DPPC/DPPS multilayer before the incorporation of the TDP, the single, ordered lamellar orientation of the lipid/TDP multilayer was significantly disturbed by the incorporation of the TDP peptide. For the pure DPPC multilayer, the incorporation of the TDP peptide had nearly no effect on the bilayer thickness, but in the mixed DPPC/DPPS multilayer system with the same P/L ratio of 1:200, the strong interaction between TDP and DPPS decreased the bilayer thickness. With increasing DPPS content, incorporation of the TDP peptide induced a phase separation at a certain concentration of DPPS. The refined XR data suggested that the TDP peptide was inserted into the hydrophobic region, indicating that TDP insertion into the membrane had occurred. Since no serious effect (e.g., membrane thinning or phase separation) was observed for the pure DPPC, the strong binding affinity of TDP for DPPS must be a key step in the CPP insertion mechanism for a plasma cell membrane.

ACKNOWLEDGMENTS

This work was supported by the Mid-career Researcher Program (Grant No. 2011-0017539), the Nuclear Research R & D Program, the Nano/Bio Science & Technology Program (Grant No. 2005-01333), PET Converging Research Center Program, and a GIST-NCRC grant (Grant No. R15-2008-

006) funded by the Ministry of Education, Science and Technology.

- ¹K. Simons and D. Toomre, *Nat. Rev. Mol. Cell Biol.* **1**, 31 (2000).
- ²Z.-J. Cheng, R. D. Singh, D. L. Marks, and R. E. Pagano, *Mol. Membr. Biol.* **23**, 101 (2006).
- ³D. A. Brown and E. London, *Annu. Rev. Cell Dev. Biol.* **14**, 111 (1998).
- ⁴M. Edidin, *Annu. Rev. Biophys. Biomol. Struct.* **32**, 257 (2003).
- ⁵M. Nielsen, L. Miao, J. H. Lisen, K. Jørgensen, M. J. Zuckermann, and O. G. Mouritsen, *Biochim. Biophys. Acta* **1283**, 170 (1996).
- ⁶M. L. Kraft, P. K. Weber, L. M. Longo, I. D. Hutcheon, and S. G. Boxer, *Science* **313**, 1948 (2006).
- ⁷J. Huang and G. W. Feigenson, *Biophys. J.* **65**, 1788 (1993).
- ⁸J. Huang, J. E. Swanson, A. R. G. Dibble, A. K. Hinderliter, and G. W. Feigenson, *Biophys. J.* **64**, 413 (1993).
- ⁹T. G. Anderson and H. M. McConnell, *Biophys. J.* **81**, 2774 (2001).
- ¹⁰C. R. Safinya, *Curr. Opin. Struct. Biol.* **11**, 440 (2001).
- ¹¹I. Koltover, T. Salditt, and C. R. Safinya, *Biophys. J.* **77**, 915 (1999).
- ¹²I. Koltover, T. Salditt, J. O. Radler, and C. R. Safinya, *Science* **281**, 78 (1998).
- ¹³H. Y. Jing, D. H. Hong, B. D. Kwak, D. J. Choi, K. Shin, C.-J. Yu, J. W. Kim, D. Y. Noh, and Y. S. Seo, *Langmuir* **25**, 4198 (2009).
- ¹⁴S. Taguchi and N. Wakayama, *Jpn. J. Appl. Phys., Part 1* **41**, 4987 (2002).
- ¹⁵F.-Y. Chen, M.-T. Lee, and H. W. Huang, *Biophys. J.* **84**, 3751 (2003).
- ¹⁶M.-T. Lee, F.-Y. Chen, and H. W. Huang, *Biochemistry* **43**, 3590 (2004).
- ¹⁷J. S. Wadia and S. F. Dowdy, *Adv. Drug Deliv. Rev.* **57**, 579 (2005).
- ¹⁸M. Green and P. M. Loewenstein, *Cell* **55**, 1179 (1988).
- ¹⁹A. Ziegler, P. Nervi, M. Dürrenberger, and J. Seelig, *Biochemistry* **44**, 138 (2005).
- ²⁰T. Harder, P. Scheiffele, P. Verkade, and K. Simons, *J. Cell Biol.* **141**, 929 (1998).
- ²¹J. E. Shaw, R. F. Epand, R. M. Epand, Z. Li, R. Bittman, and C. M. Yip, *Biophys. J.* **90**, 2170 (2006).
- ²²G. Tae, H. Yang, K. Shin, S. K. Satija, and N. Torikai, *J. Pept. Sci.* **14**, 461 (2008).
- ²³S. Ludtke, K. He, and H. Huang, *Biochemistry* **34**, 16764 (1995).
- ²⁴S. X. Hu, H. X. Li, Q. J. Jia, Z. H. Mai, and M. Li, *J. Chem. Phys.* **122**, 124712 (2005).
- ²⁵L. L. Xing, D. P. Li, S. X. Hu, H. Y. Jing, H. L. Fu, Z. H. Mai, and M. Li, *J. Am. Chem. Soc.* **128**, 1749 (2006).
- ²⁶H. W. Huang, F.-Y. Chen, and M.-T. Lee, *Phys. Rev. Lett.* **92**, 198304 (2004).
- ²⁷W. H. Huang, *Biophys. J.* **50**, 1061 (1986).
- ²⁸S. J. Ludtke, K. He, W. T. Heller, T. A. Harroun, L. Yang, and H. W. Huang, *Biochemistry* **35**, 13723 (1996).
- ²⁹H. W. Huang, *Biochemistry* **39**, 8347 (2000).
- ³⁰M. R. Horton, C. Reich, A. P. Gast, J. O. Rädler, and B. Nickel, *Langmuir* **23**, 6263 (2007).